EVS24
Stavanger, Norway, May 13-16, 2009

Experimental Research on Wheel Slip Control for the HEV In-Wheel Motor along the Rough Terrain with Rectangular Obstacles

Jeong Il Seo[1], Kyogun Chang[2], Soon Kyu Jung[2], Hyun Seok Choi[2], Jae Yong Kim[2], and Dong Hyun Kim[2]
[1]*Agency for Defense Development, Yuseong P.O. Box 35-53, Daejeon, 305-600, Korea, jiseo@add.re.kr*
[2]*Agency for Defense Development, Yuseong P.O. Box 35-53, Daejeon, 305-600, Korea*

Abstract

This paper presents experimental approach for a longitudinal wheel slip control scheme of the in-wheel motorized driving systems applied in the military series hybrid electric vehicles. Research on slip mechanism between a tire and ground needs to be modeled and simulated, to secure better vehicle driving performance in the field. Especially the effect of diverse gravels has to be precisely defined. A test rig is designed to test driving performances and to understand tire slip mechanism. The modeling and simulation results presented will be compared with experimental results by the test rig mimicking rectangular obstacles with different height. Based on modified modeling of tire slip mechanism, a wheel slip control to improve vehicle driving performance in the rough terrain with rectangular obstacles will be proposed.

Keywords: list 3-5 keywords from the provided keyword list in 9,5pt italic, separated by commas

1 Introduction

In recent years, great attention has been gradually shown to the development of HEV(Hybrid Electric Vehicle), EV(Electric Vehicle), or FCEV(Fuel-Cell Electric Vehicle) to reduce energy consumption with low carbon, as oil price has been steeply increased and environment pollution has been socially issued. As a part of these trends, ADD(Agency for Defense Development) recently developed the Dog-Horse robot(Fig.1) equipped a series hybrid electric power-train system[1]. The robot can be driven by 6 in-wheel motors which are located inside tire rims.

The in-wheel motorized driving system is generally applied in the military series hybrid electric vehicles. It does have the advantage of providing high qualified driving performance in rough terrain. The in-wheel motor transfers electric power from a battery to mechanical angular velocity and torque which finally drive tire and the robot. The major advantage of this system is that it provides high qualified driving performance in rough terrain. However, vehicle driving control for the in-wheel motorized driving system is relatively difficult because the vehicle is very prone to be dynamically unstable unless real-time responses about external complex disturbances are responded. Its unstable driving causes unnecessary energy losses.

Therefore, research on wheel slip control to prevent avoidable slip and to maximize vehicle driving performance is clearly required. For an initial step of this research, slip mechanism and wheel slip control for the HEV in-wheel motor along even roads and rough terrain with diverse rectangular obstacles.

Figure1 : The Dog-Horse Robot

Zegelaar and Pacejka[2] proposed the rigid ring model to model the tire rolling over unevenness. They provided simulation results of the dynamic behavior of the tire. Pacejka[3] suggested the two-point follower technique and the 'Tandem Egg' technique which was initially reported by Schmeitz[4].

Triche, et al.[5] provided experiments to determine design requirements against shock load for the in-wheel motor. The experimental results showed the in-wheel motor would be experienced over 150 g's with a 10 to 20 ms pulse width. However, they did not provide experimental results in a real in-wheel motor system.

This paper is divided into three parts: 1) bases of vehicle dynamic model, 2) experimental objects and the test rig designed, and 3) experimental results and discussion. This paper attempts to model and simulates behavior of slip ratio and rolling resistance when an in-wheel motorized driving system moves along even surface or rough terrain with rectangular obstacles such as gravels. After executing experiments with different heights of rectangular obstacles, experimental results and simulation results will be compared and then characteristic parameters of simulated slip mechanism between the wheel and ground will be modified.

2 TIRE SLIP MECHANISM

The in-wheel and tire driving model is discussed in this chapter. To develop the model, the longitudinal dynamics of the vehicle has to be defined with external force inputs. First, experimental objects are described in next section.

2.1 In-wheel Motor and Tire

Experimental object, the in-wheel motor system of the Dog-Horse robot, is shown in Fig.2. The motor system includes in-wheel motor, tire, rim, and gear train. The system has to absorb impacts from rough roads or fields and minimizes effects of those impulsive forces. In addition, it effectively has to release generated heat

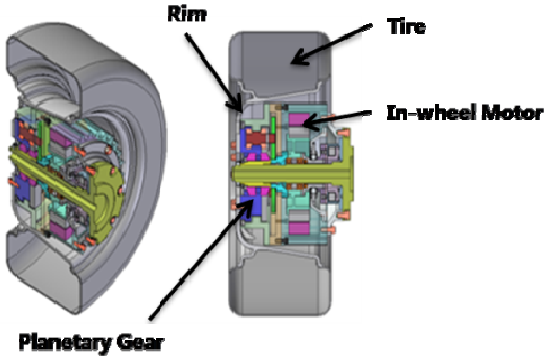

Figure2 : The In-Wheel Motor System

The in-wheel motor has to generate the same torque-velocity characteristics as those to satisfy vehicle mobility. The driving characters can be generally implemented by field weakening motor control, which is one of the inner-loop torque control methods. To detect precise angular velocity, one resolver is equipped inside the in-wheel motor whose type is an IPMSM (Interior Permanent Magnet Synchronous Motor) to increase torque density per volume. For safety, two thermal sensors are attached to the motor stator and IGBT of the motor inverter.

Dunlop's KT 403 tire is selected to endure steady mobility in the rough terrain. The tire is a type of ATV's tires. Aluminum rim for each wheel is specially machined.

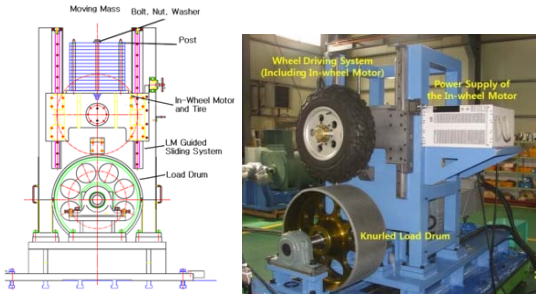

Figure3 : In-Wheel Motorized System and Load Drum of the Test Rig

Fig.3 shows the test rig to measure driving performances such as braking distance, system efficiency, temperature saturation curve, and T-N curve, and to modify modeling of tire slip mechanism. The load drum in Fig.3 is driven by an AC motor selected real-time speed control mode or torque control mode. In Fig.3, the surface on the load drum is knurled and its radius is 0.33m. To implement the inertia effect from vehicle along the vertical direction, a vertical moving mass loads on the in-wheel motorized driving system. The weight of the moving mass in the normal direction is 237kgf.

2.2 Dynamics Model of Tire and Load Drum

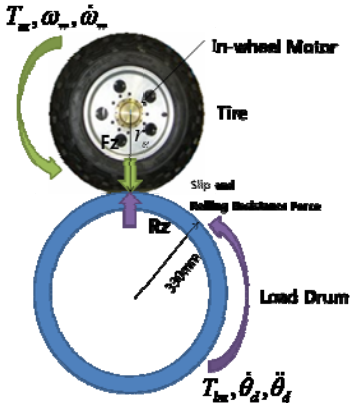

Figure4 : Dynamic Motion of Tire and Load Drum

When a driving torque of the in-wheel motor is applied to a pneumatic tire, the tractive force ($F_{tx} = r_e F_z(\mu + f_r)$) is developed at the tire-ground contact patch. The longitudinal dynamic models can be modeled by Fig.4. Dynamic motion driven by an in-wheel motor can be described by

$$I_w\dot{\omega}_w = T_m - T_{mf} - r_e F_z(\mu + f_r)$$
$$I_{ld}\ddot{\theta}_{ld} = T_l - T_{lf} - r_{ld}(\mu + \frac{e}{r_{lm}})F_z \quad (1)$$

, where I_w is the mass moment inertia of the wheel about the axis of rotation, ω_w the angular velocity of the tire, T_m the motor torque generated by the in-wheel motor, F_z the normal force, f_r , or $\frac{e}{r_e}$, the coefficient of rolling resistance, e is the eccentric distance from wheel axis to the acting point of the normal force, μ coefficient of friction which is the function of slip ratio(s) and contact length in the contact patch, and r_e the effective radius of a tire. T_l is the torque of the load motor, I_{ld} is the equivalent moment inertia at the load drum, and $\ddot{\theta}_d$ is the angular acceleration of the load drum. In (1), T_{mf} and T_{lf} are friction torques of the wheel side and the load drum side, respectively. However, those values are small enough because of calibration so T_{mf} and T_{lf} are ignored.

The effective radius(r_e) in (1) of a tire can be expressed by

$$r_e = r_{e0}\frac{F_z}{K_t} \quad (2)$$

,where r_{e0} is the original radius of the tire and K_t is the transitional stiffness of the tire. However, the effective radius can be calculated from the ratio between wheel speed and load drum speed because the radius of metal load drum can be assumed constant.

Gillespie[6] described coefficient of rolling resistance(f_r) as the function of vehicle speed:

$$f_r = f_0 + f_s\left(\frac{\upsilon_{xw}}{100}\right)^{2.5} \quad (3)$$

,where f_0 is basic coefficient and f_s is speed effect coefficient. Both parameters depend on pressure of the tire. υ_{xw} (m/sec) is the speed of the wheel center in the proceeding direction.

Slip ratio can be defined in terms of braking or accelerating. Slip ratio is given by

$$s = \frac{r_e\omega - V_x}{V_x}(braking)$$
$$s = \frac{r_e\omega - V_x}{r_e\omega}(accelerating) \quad (4)$$

,where V_x is the proceeding velocity of the vehicle [6][7].

The tire-road friction coefficient(μ) in (1) is defined as the ratio of the frictional force (F_{fric}) acting in the wheel plane and the normal force, F_z :

$$\mu = \frac{F_{fric}}{F_z} \quad (5)$$

The friction coefficient can be formulated by the method of Burckharht[8].

$$\mu(s_i) = c_1[1 - \exp(-c_2 s)] - c_3 s \quad (6)$$

, where s is the slip ratio measured.

2.3 Slip Models of Rolling over Rectangular Obstacles

As seen in Fig.5, after the wheel meets a rectangular obstacle, the wheel will float in the air. As a result, all motor torque will transform into inertia torque and the angular velocity of the wheel will be steeply increased. After contact between

the wheel and ground, the effective radius, slip ratio and contact length in the contact patch will be changed and slip will be generated by sudden changes of the tractive force.

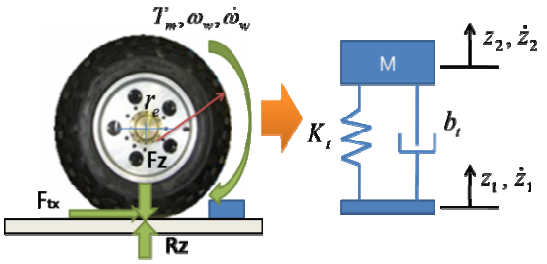

Figure5 : Rigid Ring Model in the Vertical Direction

The normal force and the tire can be modeled by a spring, a mass, and a damper(Fig.5). The normal force can be obtained by :

$$F_z = b_t(\dot{z}_1 - \dot{z}_2) + K_t(\dot{z}_1 - \dot{z}_2) \quad (7)$$

, where b_t is the coefficient of transitional damping and K_t is the transitional stiffness of the spring model.

3 EXPERIMENTS and DISCUSSION

3.1 Experimental Test Rig

A similar test rig to Fig.3 which could test performances of the active suspension system was proposed by Beno, et al.[9] but their focus was to test performances of active suspension system newly developed. On the other hand, ADD developed test-bed to test performances, such as temperature behavior in the driving environment, T-N curve, efficiency, minimum braking distance and so on, of the in-wheel motor system. In addition, ADD's test rig can verify slip mechanism and its information help better motor control system developed.

Dynamic experiments of slips between the tire and the load drum are executed in drum type dynamometer system as shown in Fig.3. The surface on load drum in Fig.3 was machined with knurling which can generate appropriate friction without unnecessary slip between tire and load drum.

Fig.7 shows basic structure of the test rig. NI PXI controller gives commands to in-wheel motor controller by CAN protocol and the load motor of the test rig and measures signals from sensors such torque sensors, a resolver and temperature sensors.

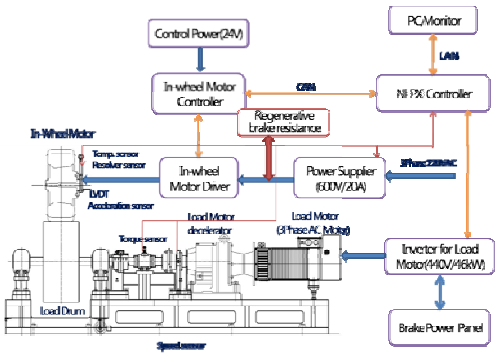

Figure7 : Structure of the Test-bed

3.2 Experimental Results

From free rolling in the test rig (Fig.3), effective rolling radius of the tire whose air pressure is 18 psi is 0.275m. Basic coefficient and speed effect coefficient of (3) are calculated by curve fitting (Fig.8): $f_0 = 0.052$ and $f_s = 2.729$. Substituting (3) is obtained by

$$f_r = 0.052 + 2.729\left(\frac{\upsilon_{xw}}{100}\right)^{1.5} \quad (8)$$

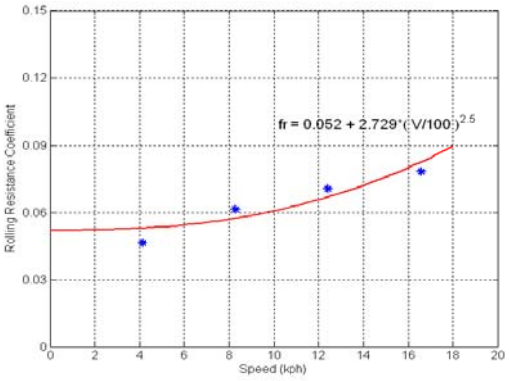

Figure8 : Longitudinal Slip Control Model

Coefficient of rolling resistances are the range of 0.05~0.09. The coefficient is more than the coefficient of the case of tractor driving on the medium hard road.

Parameters, c_1, c_2 and c_3, of (6) can be calculated by curve fitting (Fig.9).

To test characteristics, b_t and K_t of equation (7), suspension test-bed (Fig.10) was utilized. The tire was oscillated by a hydraulic actuator.

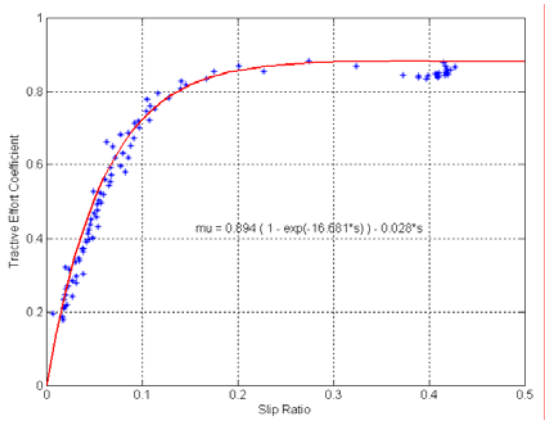

Figure9 : Tractive Friction Coefficient v.s Slip Ratio

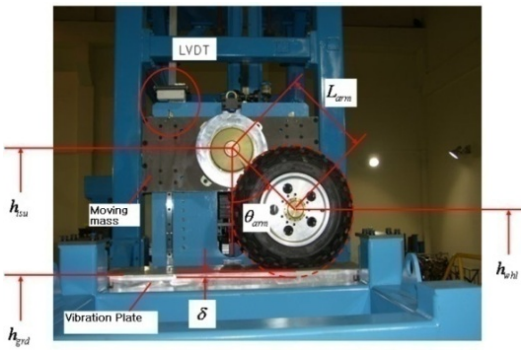

Figure10 : Test-bed for the Tire Characters

At low oscillation with 5Hz, experimental result is shown in Fig.11 with simulation data of $b_t = 1{,}500 N_s/m$ and $K_t = 120{,}660 N/m$. The simulation data behaves similar to experimental result in Fig.11.

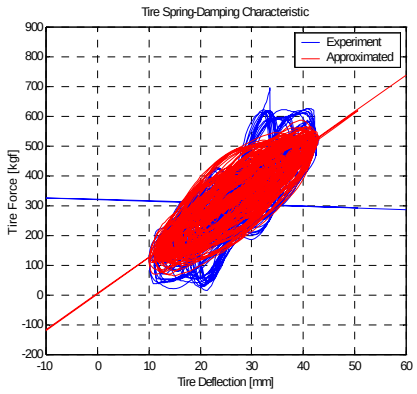

Figure11 : Test Results for Tire Characteristics

3.3 Discussion

Basic parameters of dynamics model of tire and load drum were obtained by experiments. Fig.12 shows proposed longitudinal slip control model. In Fig.12, s_r is the reference of slip ratio and s is actual slip ratio in the system. Γ is electric flux. T_m^* is the torque command of the field weakening controller and is calculated from rolling resistance and friction force models of (3) and (5).

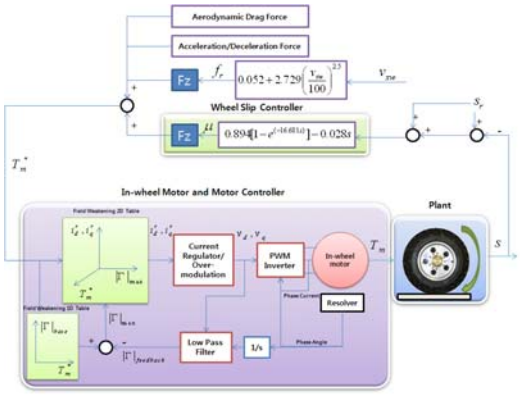

Figure12 : Longitudinal Slip Control Model

Field weakening control scheme and space vector PWM method for driving the in-wheel motor of the Dog-Horse robot are applied[10]. Therefore, the torque command(T_m^*) is converted into current commands by the field flux-torque-current table. The current commands drive in-wheel motor to generate desired torques. T_m is the output torque from the in-wheel motor. The plant in Fig.12 describes the mechanism where the longitudinal tire tractive force($F_{tx} = r_e F_z(\mu + f_r)$) is generated by slip ratio(s) and the coefficient of rolling resistance in the contact patch.

4 CONCLUSION

This paper suggested experimental approach of a longitudinal wheel slip control scheme for the in-wheel motorized driving systems. Behavior of tire longitudinal slip mechanism was modeled and tested. Experimental results by the test rig mimicking rectangular obstacles with different height were compared to simulation results. Based on modified modeling of tire slip mechanism, a wheel slip control for vehicle driving performance in the rough terrain with rectangular obstacles was discussed. As future work, the control scheme will be simulated, tested, and applied in the motor inverter of the Dog-Horse robot.

References

[1] K. Chang, H. Choi, Y.-W. Kim, and Y.-B. Lee, "Development of the Military In-wheel Motor Dynamometer for a HEV," KSAE 2008 Annual Conference Proceedings, 2008. Nov.

[2] P.W.A. Zegelaar and H.B. Pacejka, "The In-plane Dynamics of Tyres on Uneven Roads," Vehicle System Dynamics Supplement 25, pp. 714-730, 1996.

[3] H.B. Pacejka, Tyre and Vehicle Dynamics, Butterworth-Heinemann, 2002.

[4] A.J.C. Schmeitz, S.T.H. Jansen, H.B. Pacejka, J.C. Davis, N.N. Kota, C.G. Liang, and G. Lodewijks, "Application of a Semi-empirical Dynamic Tire Model for Rolling over Arbitrary Road Profiles," Int. J. of Vehicle Design, vol 36., pp. 194-215, 2004.

[5] E. Triche, Jr. J.H. Beno, M.T. Tims, M. Worthinton, and J. Mock, "Shock Loading Experiments and Requirements for Electric Wheel Motors on Military Vehicles," SAE International, 2005.

[6] T.D. Gillespie, Fundamentals of Vehicle Dynamics, SAE, Inc., PA, 1992.

[7] J. Y. Wong, Theory of Ground Vehicles 3rd Ed., John Wiley and Sons, Inc., 2001.

[8] U. Kienche and L. Nielsen, Automotive Control Systems, Society of Automotive Engineers, USA., 2000.

[9] J.H. Beno, M.T. Worthington and J.R. Mock, Suspension Trade Studies for Hybrid Electric Combat Vehicles, SAE 2005-01-0929, 2005

[10] S.-M. Kim, Y.-H. Park, S.-K. Sul, K.-Y. Choi, K. Chang, and C.K. Song, "Flux-Weakening Control of In-Wheel Motor for Traction of DHV," Conf. of 15th Ground Military System Development, 2007.